A Probabilistic Model-Based Prognostics Using Meshfree Modeling: A Case Study on Fatigue Life of a Cantilever Beam

Conference Paper · November 2016

DOI: 10.1115/IMECE2016-67936

CITATION
1

READS
165

4 authors, including:

Haileyesus Endeshaw
Texas Tech University
16 PUBLICATIONS **65** CITATIONS

SEE PROFILE

Fisseha M. Alemayehu
West Texas A&M University
41 PUBLICATIONS **210** CITATIONS

SEE PROFILE

Joao Paulo Dias
Shippensburg University
44 PUBLICATIONS **177** CITATIONS

SEE PROFILE

Proceedings of the ASME 2016 International Mechanical Engineering Congress and Exposition
IMECE2016
November 11-17, 2016, Phoenix, Arizona, USA

IMECE2016-67936

A PROBABILISTIC MODEL-BASED PROGNOSTICS USING MESHFREE MODELING: A CASE STUDY ON FATIGUE LIFE OF A CANTILEVER BEAM

Haileyesus B. Endeshaw
Texas Tech University
Department of Mechanical Engineering
Lubbock, Texas, USA

Fisseha M. Alemayehu
West Texas A&M University
School of Engineering, Computer Science and Mathematics
Canyon, Texas, USA

Stephen Ekwaro-Osire
Texas Tech University
Department of Mechanical Engineering
Lubbock, Texas, USA

João Paulo Dias
Texas Tech University
Department of Mechanical Engineering
Lubbock, Texas, USA

ABSTRACT

Accurate prediction of remaining useful life (RUL) will improve reliability and reduce maintenance cost. Therefore, prognostics is essential to predict the RUL of systems and components. However, a big issue of uncertainty prevails in prognostics due to the fact that prognostics pertains to prediction of future state, which is affected by uncertainty. While various researches have been done in areas of prognostics and health management, they lack to perform RUL predictions efficiently. There is a need for an efficient comprehensive framework for quantifying uncertainty in prognostics. The research question to this study is: can meshfree modeling be used in probabilistic prognostics to efficiently predict RUL? The specific aims developed to answer the research question are (1) develop a computational framework for probabilistic prognostics of a fatigue life of a component using meshfree modeling, and (2) perform case study analyses on fatigue life of a cantilever beam. A probabilistic framework was developed that efficiently predicts the RUL of a component using a combination of the meshfree method known as local radial point interpolation method and a fatigue degradation model. Loading uncertainty is quantified and employed in the framework. The computational framework is easily customizable and computationally efficient and, hence, aids in decision making and fault mitigation. As a case study, the RUL of a cantilever beam under plane stress subjected to fatigue loadings was analyzed. Uncertainties in the RUL were quantified in terms of probability density functions, cumulative distribution functions, and 98% bounds of confidence interval. Sensitivity analysis was studied and computational efficiency of the framework was also investigated using first order reliability method and Monte Carlo method. When compared to the Monte Carlo method, first order reliability method provides reasonably good results and is found to be computationally more efficient.

Key words: *Prognostics, remaining useful life, uncertainty, meshfree, probabilistic*

INTRODUCTION

Background

Prognostics and Health Management

The cost of operation and maintenance of a system accounts for a great portion of the total cost associated with the system [1]. This cost can be reduced by making appropriate failure predictions in advance. Health management refers to instantaneous health monitoring of a system, whereas prognostics is the prediction of future states of a system or a component to predict the remaining useful life [2–4]. The initial input data to prognostics comes from diagnosis [2]. Generally, prognostics follows two important steps namely, state estimation using Bayesian tracking and future state prediction [5].

Prognostics methodologies can be categorized into model-based, statistical data driven, and hybrid methods [6, 7]. Data driven methods build relationship between measured data and the state of a system using machine learning and pattern recognition methodologies [8]. Data driven method shows that the results of a purely data driven approach without the physical model results in a high uncertainty values and is inconvenient for long term predictions [9]. An extensive review of statistical data driven approaches is provided by Si et al. [10]. A review of state of the art prognostics approaches and challenges regarding rotary machinery is presented in [11]. Model-based approaches implement mathematical formulations to approximate the physics of the system for RUL prediction [8]. Hybrid methodologies use the combination of model-based and data driven approaches [6]. Studies on data driven approaches can be found in [8] and [12]. Detail review on common model-based and data-driven algorithms and their advantages and disadvantages can be found in [13]. Another type of

classification of prognostics is testing-based and condition-based [3, 14]. Testing based or offline prognostics is performed before and/or after operation whereas condition-based (online) prognostics refers to performance monitoring during operation. Sikorska et al. [15] classified prognostics modeling methods as knowledge-based, life expectancy, artificial neural networks, and physical models and presented an extensive review on selection of prognostics modeling techniques in industry. Saxena et al. [16–18] studied the performance of various prognostics algorithms and proposed a metric for evaluating such algorithms.

Since prognostics refers to predicting future state of a system, it is necessary to consider uncertainties to account for eminent variability [19, 3, 20]. There are various sources of uncertainty that should be considered in prognostics [3, 21]. Sources of uncertainty include sensor and measurement errors, state estimates, future loading conditions, and environmental conditions [22]. Of these sources of uncertainties, future loading is the most challenging in prognostics [5, 23]. Another classification of sources of uncertainty is present uncertainty, future uncertainty, modeling uncertainty and prediction method uncertainty [22, 5]. It should also be important to know that RUL prediction of prognostics should be expressed as a distribution with a given confidence interval instead of a specific life estimate [15]. It should be based on this confidence interval that business decisions should be made [15]. Sankararaman et al. [23] studied the application of FORM methods for uncertainty quantification in prognostics for applications of online health monitoring.

Modeling

Finite element method (FEM) has been used widely for problems which do not have a closed form solution. However, FEM is not without limitations. The first limitation is FEM causes the problem of re-meshing in crack propagation problems. Re-meshing in FEM is necessary due to the arbitrary and complex path of crack propagation which causes misalignment with the edge of the finite elements and, hence, causes discontinuous displacement fields to be created within the elements [25, 33–35]. Thus, re-meshing makes finite element (FE) computation cumbersome and computationally expensive [28]. Another limitation of FEM is the fact that its applicability is low in problems where mesh distortions might be available since FEM does not work well with distorted meshes [27]. Other limitations of FEM include loss of accuracy in large deformations, low accuracy of stresses at element interfaces caused by the assumption of continuous displacement field during FEM formulation [29]. To overcome some of the problems of FEM, the extended finite element method (X-FEM) was developed. Bordas et al. [30] presented a C++ open source framework for X-FEM, compiled by Visual Studio. While X-FEM avoids the issue of re-meshing in FEM, its derivatives lack smoothness and also suffers from the inability of handling distorted meshes very well [27].

Meshfree methods (also known as meshless methods) were formulated to avoid some of the issues associated with finite element (FE) approximations; i.e. issues caused by reliance on mesh. Meshfree methods were applied in areas of solid mechanics, fluid dynamics, and astrophysics [27]. Unlike FE methods, meshfree methods do not depend on predefined mesh to generate system of algebraic equations for the problem domain [31]; instead, meshfree methods use nodes (also known as field nodes) for approximation [35, 37]. The quality of higher order of continuity in meshfree methods becomes especially very beneficial in problems with discontinuities, such as cracks, and they can easily model problems with moving discontinuities such as crack propagation and phase transformation [27]. Some of the most common meshfree methods include smooth particle hydrodynamics method, element-free Galerkin (EFG) method [32], reproducing kernel particle method (RKPM), radial point interpolation method (RPIM), and meshless local Petrov-Galerkin (MLPG) method [33]. Meshfree methods can be classified based on: formulation methods (local weak-forms, global weak-forms, and collocation techniques), function approximation methods (moving least squares (MLS), integral representation, point interpolation methods), and domain representation (domain-type and boundary-type methods) [29]. EFG and RKPM are based on global weak-forms, whereas MLPG method is based on local weak-forms. Meshfree methods which are based on global weak-forms require background cells to perform integration, whereas those that are based on local weak-forms employ quadrature domains for integration. Local meshfree methods use the so-called support domains for the sake of interpolation. Thus, interpolation will be based on field nodes inside the support domain.

Degradation Models

Degradation models are used to estimate future states and RUL of a system or a component based on available data. One of the most popular degradation models is capacity degradation model of a battery [3, 23]. This degradation model is popular among several researchers because it is straightforward and, hence, convenient to demonstrate RUL prediction. An et al. [7] employed a simplified power law model to demonstrate estimation of battery life; Eq. (1) shows the battery degradation model:

$$x_k = e^{(-b\Delta t)} x_{k-1} \tag{1}$$

where x is the capacity, the subscript k is the time step, b is the model parameter, and Δt is the time interval. Another popular degradation model is the discretized form of Paris' law (see Eq. (2)), which is used recursively to predict future crack sizes based on previous crack size estimate [7, 13, 47, 55].

$$a_k = a_{k-1} + C(\Delta K)^m \Delta \mathrm{N} \tag{2}$$

where a is the crack size, ΔN is the number of cycles, ΔK is the stress intensity factor and C and m are material parameters. Correlation between C and m and their joint probability density function (PDF) with different levels of noise inputs was studied by An et al. [36]. They reported that the correlation between the parameters is influenced by the level of noise imparted into the

system. Recently, a study on the improvement of Paris' law was proposed by Leiting et al. [37]. Profound discussion on the dynamics of crack growth could be found in [38]. Other degradation models include material wear of a pneumatic value [39] and material degradation due to fatigue damage [40]. Fatigue life of a component under cyclic loading can be given by

$$N = \left(\frac{\sigma_a}{a_f}\right)^{1/b_f} \quad (3)$$

where σ_a is a cyclic stress and a_f and b_f are the model parameters that are updated according to Manson's method of cumulative fatigue damage (CFD) [40].

Probabilistic Analysis

Data collection usually imparts some degree of uncertainty and most engineering parameters are random in nature, i.e. they have a certain degree of uncertainty. As a result, the performance of the system cannot be exactly determined; instead, it is expressed in terms of probability. The probability of ensuring a desired performance is reliability [41]. Traditional deterministic design approaches do not consider uncertainty, whereas probabilistic analysis involves quantification of uncertainty and determining the reliability or the probability of failure of an engineering system [42]. Probabilistic study involves gathering relevant information and expressing it mathematically to obtain the PDF and the cumulative distribution function (CDF). Probabilistic analysis involves selection of random variables in the mathematical model, quantifying their uncertainty and analyzing their effect on the response parameter. Uncertainty quantification may involve sampling methods or analytical methods. Sampling methods include Monte Carlo (MC), and Latin hypercube sampling (LHS), whereas analytical methods include first-order second moment method (FOSM), first-order reliability method (FORM), and second order reliability method (SORM). Analytical methods employ limit state functions to calculate the probability of failure [23]. The probabilistic analysis software NESSUS performs probabilistic and sensitivity analyses using both analytical and sampling methods.

Consideration of uncertainty is critical in ensuring reliability of systems, such as wind turbine gearboxes [43]. Probabilistic analysis is important in real-world applications where dynamic loads are prevalent [41]. It was reported that wind turbine reliability analysis is essential since wind turbines experience variable torsional and non-torsional loads and uncertain parameters prevail in the stage of manufacturing and assembly [44]. The importance of uncertainty consideration in wind turbine gearbox was demonstrated in [65, 66, 68].

Remaining Useful Life Prediction

In model-based prognostics, RUL prediction involves steps of filtering of observed data and implementation of degradation model for state estimation. As long as there are available data, state estimation involves filtering procedure. However, once available data has been used, state estimation will be based solely on the physics of the problem, i.e. the degradation model. A criteria for end of life should be implemented [7]. Sankararaman et al. [23] presented a methodology for predicting the RUL of a lithium-ion battery using a probabilistic approach for uncertainty quantification. They implemented FORM to analyze the different sources of uncertainty including loading uncertainty and state uncertainty. The reduction in uncertainty with time was depicted by converging bounds of 98% confidence level [23]. Other researchers employed prognostics of fatigue crack propagation of a gear using gear dynamics model and FEM analysis to determine RUL [46]. Si et al. [10] outlined challenges regarding prediction of RUL. The first challenge is concerning the development of model-based RUL prediction for systems. The authors argued that model-based estimation is especially important in cases where no measured data is available. Secondly, there is a challenge of integrating multi-dimensional data from condition monitoring. The third challenge lies in accurately modeling external variables such as loadings and environmental conditions, for accurate RUL prediction. The last challenge mentioned is development of a model for RUL prediction for multiple failure scenarios of a component.

Motivation

The traditional schedule-based maintenance is not capable of predicting failure accurately. As a result, the status of the system may severely deteriorate and eventually may result in system downtime [6]. This is especially apparent in wind turbine gearbox system, which often fails before its expected lifetime [45]. While uncertainty consideration is necessary in diagnosis, the importance of quantifying uncertainty significantly increases in prognostics since prognostics involves predicting future state, which is even more uncertain [23]. Sources of uncertainties in prognostics include measurement, modeling, material property, and future loading [21, 22]. The process of prognostics should, thus, account for these uncertainties and provide a PDF of RUL rather than a scalar value of the RUL estimate [6]. While various researches have been done in areas of prognostics and health management, they lack to perform RUL predictions efficiently. There is a need for a comprehensive framework for quantifying uncertainty in prognostics [22, 5]. Accurate prediction of RUL will improve reliability and reduce the maintenance cost [47]. Model-based prognostics method was selected since there is a need of physics-based models in cases where sufficient measured data is not readily available [15, 10]. A meshfree method is selected for modeling since its use can be extended to discontinuous structures such as cracks, which are more efficiently modeled using meshfree methods than FEM [33, 35, 37].

Research Question and Specific Aims

This study answers the research question: can meshfree modeling be used in probabilistic prognostics to efficiently predict RUL? The following specific aims were developed to answer the research question: (1) develop a computational framework for probabilistic prognostics of a fatigue life of a

component using meshfree modeling, and (2) perform case study analyses on fatigue life of a cantilever beam.

METHODOLOGY

Meshfree Modeling

For a problem of domain Ω, the local weighted residual form over a quadrature domain Ω_q is given by [29]

$$\int_{\Omega_q} \widehat{\boldsymbol{W}}_I \, (\sigma_{ij,j} + \, b_i) \, d\Omega = 0 \tag{4}$$

where $\widehat{\boldsymbol{W}}$ is the weight function at node I, σ_{ij} is the stress and $\sigma_{ij,j} = \partial\sigma_{ij}/\partial x_j$, and b is the external force vector. The relaxed weak form of Eq. (4) can be written as

$$\int_{\Omega_q} \widehat{\boldsymbol{W}}_{I,j}\sigma_{ij} \, d\Omega - \int_{\Gamma_{qi}} \widehat{\boldsymbol{W}}_I t_i \, d\Gamma - \int_{\Gamma_{qu}} \widehat{\boldsymbol{W}}_I t_i \, d\Gamma = \int_{\Gamma_{qt}} \widehat{\boldsymbol{W}}_I \bar{t}_i \, d\Gamma + \int_{\Omega_q} \widehat{\boldsymbol{W}}_I b_i \, d\Omega \tag{5}$$

where t is the traction on the boundary and Γ_{qi}, Γ_{qu} and Γ_{qt} are the boundaries of the quadrature domain which does not intersect with the global boundary, Γ, which intersects with the essential boundary, and which intersects with the natural boundary, respectively. The discretized form of Eq. (5) could be obtained by representing the problem domain, Ω, by distributed field nodes. The stress at a point in the problem domain is given by

$$\boldsymbol{\sigma}_{(3\times1)} = \boldsymbol{D}_{(3\times3)}\boldsymbol{\varepsilon}_{(3\times1)} = \boldsymbol{D}_{(3\times3)}\boldsymbol{B}_{(3\times2n)}\boldsymbol{u}_{(2n\times1)} \tag{6}$$

where $\boldsymbol{n}$ is the number of field nodes in the support domain, $\boldsymbol{u}$ is the displacement of the point, $\boldsymbol{\varepsilon}$ is the strain, and $\boldsymbol{D}$ is the matrix of elastic constants and $\boldsymbol{B}$ is the strain matrix, which is given by

$$\boldsymbol{B}_{(3\times2n)} = \begin{bmatrix} \frac{\partial\varphi_1}{\partial x} & 0 & \dots & \frac{\partial\varphi_n}{\partial x} & 0 \\ 0 & \frac{\partial\varphi_1}{\partial y} & \dots & 0 & \frac{\partial\varphi_1}{\partial y} \\ \frac{\partial\varphi_1}{\partial y} & \frac{\partial\varphi_1}{\partial x} & \dots & \frac{\partial\varphi_n}{\partial y} & \frac{\partial\varphi_n}{\partial x} \end{bmatrix} \tag{7}$$

where φ is the shape function and the index associated with it is the field node. Substituting Eq. (7) into Eq. (6), the discretized system of equations can be written as

$$\int_{\Omega_q} \boldsymbol{V}_I\boldsymbol{D}\boldsymbol{B}\boldsymbol{u} \, d\Omega - \int_{\Gamma_{qi}} \widehat{\boldsymbol{W}}_I\boldsymbol{n}\boldsymbol{D}\boldsymbol{B}\boldsymbol{u} \, d\Gamma - \int_{\Gamma_{qu}} \widehat{\boldsymbol{W}}_I^T\boldsymbol{n}\boldsymbol{D}\boldsymbol{B}\boldsymbol{u} \, d\Gamma = \int_{\Gamma_{qt}} \widehat{\boldsymbol{W}}_I^T\bar{\boldsymbol{t}} \, d\Gamma + \int_{\Omega_q} \widehat{\boldsymbol{W}}_I^T\boldsymbol{b} \, d\Omega \tag{8}$$

where $\widehat{\boldsymbol{W}}$, $\boldsymbol{V}$, and $\boldsymbol{n}$ are the weight matrix, the matrix of weight derivatives, and the unit normal vector, respectively. Eq. (8) can be re-written as a matrix form as in Eq. (9)

$$(\boldsymbol{K}_I)_{2\times2n}(\boldsymbol{u})_{2n\times1} = (\boldsymbol{f}_I)_{2\times1} \tag{9}$$

where $\boldsymbol{K}_I$ is the nodal stiffness matrix of the I^{th} node and $\boldsymbol{f}_I$ is the nodal force vector. The integrals in Eq. (8) can be obtained by Gauss quadrature. Integrations are employed locally over each local quadrature domain, Ω_q, with a size of $r_q = \alpha_q d_{cl}$. The size of the local weight function Ω_w is denoted by r_w, where $r_w = r_q$ for simplicity. The size of local support domain Ω_s is given by $r_s = \alpha_s d_{cl}$, where d_{cl} is the nodal spacing and α_s and α_q are dimensionless factors to control the sizes of the support domain and the quadrature domain, respectively. All the three local domains considered are rectangular.

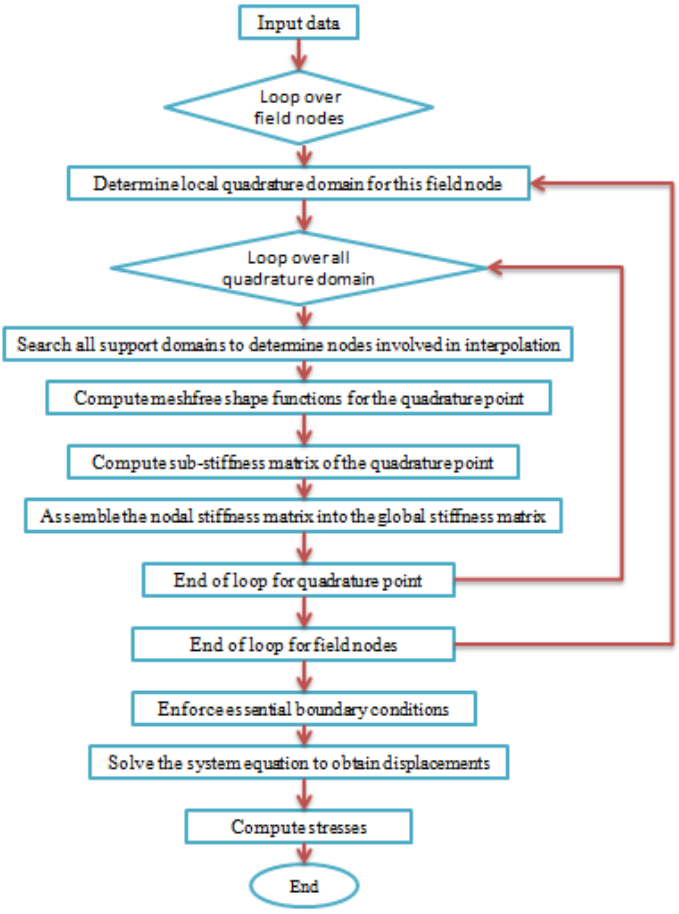

Figure 1. Flowchart of LRPIM programming [29].

A 2D cantilever beam subjected to a completely reversed cyclic loading of 10 kN was modeled using one of the meshfree methods known as local radial point interpolation method (LRPIM). LRPIM employs augmented basis functions of radial and polynomial basis functions [29]; (program flowchart is presented in (Figure 1). Detail formulation of the LRPIM can be found in [29]. Figure 2 depicts the problem domain and local quadrature domain,Ω_q, support domain, Ω_s, and weight domain, Ω_w. The meshfree program contains a number of subroutines which are responsible for computing different parts of the program. These subroutines are for computing LRPIM shape functions, quadrature domain, Gauss points, weight functions, integration of internal and essential BCs, integration of natural BCs, displacement, stress, and enforcing essential BCs. Values of the model parameters were also varied within their respective recommended ranges for best results.

The first set of input parameters for the meshfree modeling are related to the characteristics of the cantilever beam, such as the traction, *P*, the width, *B*, height, *H*, poison's ratio, υ, and the Young's modulus, *E*. The second set of inputs, which are model parameters for the meshfree modeling, is listed in Table 1.

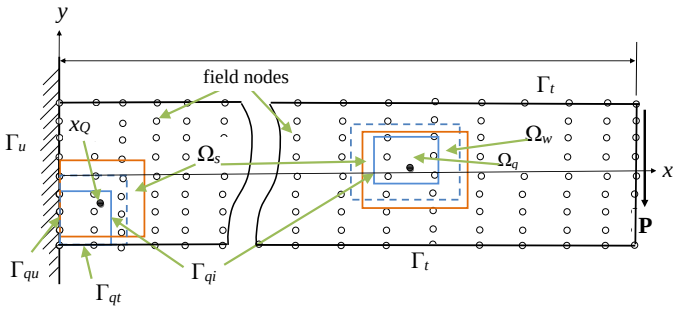

Figure 2. Cantilever beam depicting nodes, Gauss quadrature points, x_Q, quadrature domains, Ω_q, support domains, Ω_S, weight domain, Ω_W, local boundaries (Γ_{qt}, Γ_{qu}, and Γ_{qi}), and global boundaries (Γ_u and Γ_t).

Table 1. LRPIM model parameters.

Parameter	Value	Parameter	Value	Parameter	Value
α_s	3.0	α_c	4.0	*ndx*	2
α_q	1.7	*q*	1.03	*ndy*	2
α_w	3.0	*dcx*	*L*/20	*p*	3
Radial basis function	Multi-quadrics	*dcy*	*H*/8		

Fatigue Life and RUL Prediction

The relationship between dynamic loading, σ_a, and fatigue life, *N*, is given by [48]

$$\sigma_a = a_f N^{b_f} \tag{10}$$

where

$$b_f = -\frac{1}{3}\log(S_m/S_e) \tag{10 a}$$

and

$$a_f = 10^{(\log(S_m)-3b_f)}. \tag{10 b}$$

S_m is the mean stress given by $0.9S_u$ and

$$S_e = \frac{1}{2} S_u C_L C_G C_S C_T C_R \tag{10 c}$$

where C_L, C_G, C_S, C_T, and C_R are correction factors due to loading, size, surface, temperature and reliability, respectively. From Eq. 10, one can find that $N = (\frac{\sigma_a}{a_f})^{1/b_f}$. Hence, the degradation model to predict RUL is given by a piecewise function for *r* number of loading and unloading events as

$$RUL = \begin{cases} \left(\frac{\sigma_a}{a_{f,1}}\right)^{\frac{1}{b_{f,1}}} - n_c & n_c = [0, n_{c,1}] \\ \left(\frac{\sigma_a}{a_{f,2}}\right)^{\frac{1}{b_{f,2}}} - n_c & n_c = [n_{c,1}, n_{c,2}] \\ \quad . & \\ \quad . & \\ \quad . & \\ \left(\frac{\sigma_a}{a_{f,r}}\right)^{\frac{1}{b_{f,r}}} - n_c & n_c = [n_{cr-1}, n_{c,r}] \end{cases} \tag{11}$$

where n_c is the number of cycles. Eq. (11) is used to predict the RUL of a component subjected to σ_a for n_c cycles *r* number of times. Note that parameters a_f and b_f are updated in every loading case due to CFD according to Manson's rule [49].

Deterministic RUL Prediction

In deterministic RUL prediction, the degradation model subroutine then returns the expected life of the beam undergoing the given stress after a given n_c number of cycles. Eventually, the framework plots the RUL versus number of cycles to show the path of the RUL followed by the beam until failure. In case of multiple loading scenario, the framework runs in a loop repeating the above steps multiple times. Hence, with each iteration, plots of RUL versus number of cycles will be generated. After the last case of load application, the framework concatenates the RUL of each level of stress and plots them in one graph to show the path of the RUL until failure.

Probabilistic RUL Prediction

In the case of probabilistic analysis, the framework takes the maximum stress value obtained from the meshfree subroutine as a mean and a 10% standard deviation to randomly generate samples from a PDF. The samples will then be passed to the material degradation model subroutine one at a time. Using the same number of cycles of load application, n_c, the subroutine provides varying RUL values for each stress sample.

The degradation model parameters a_f and b_f of each sample stress were updated with every level of load application. Due to the randomness nature of the stress, the RUL will be a PDF at each level of load application. The median RUL and the RUL at the bounds of the 98% confidence level at each level of load application will be selected. After the application of the last loading, the framework plots these RUL values.

In order to investigate the potential of using the FORM for improved computational efficiency in the prognostics framework, probabilistic analysis was performed using NESSUS software. CDF of the initial life of the cantilever beam obtained using FORM was compared for accuracy with that of MC method with 10,000 samples. Considering σ_a and S_u as random variables, sensitivity analysis with respect to the mean and standard deviation of each random variable was also performed using NESSUS.

RESULTS AND DISCUSSION

Framework for Probabilistic Prognostics

A probabilistic prognostics framework that is capable of predicting RUL of a component under fatigue loading, both deterministically and probabilistically, was developed (Figure 3). The framework consists of LRPIM meshfree subroutines for a 2D modeling and RUL prediction program developed using MATLAB. The required input parameters to the framework are geometrical properties, material properties (elastic modulus, E, Poisson's ration, υ), applied load, P, the ultimate strength of the material, S_u, the number of cycles, n_c, and meshfree modeling parameters listed in Table 1. In addition, correction factors C_L, C_G, C_S, C_T and C_R are input parameters for the framework.

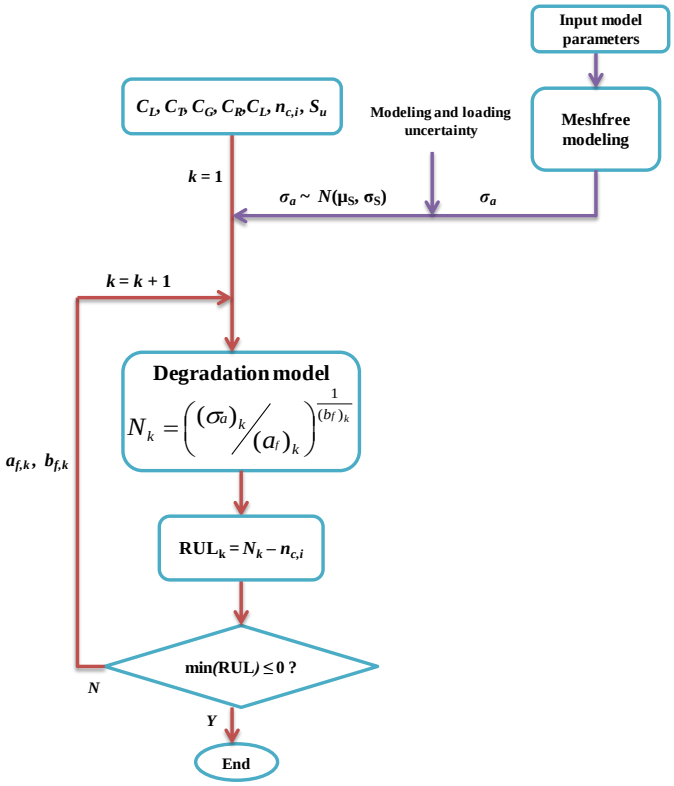

Figure 3. A framework for probabilistic prognostics of a component using meshfree modeling.

Analysis of meshfree modeling yields the maximum stress on the component. In order to determine the stress, the meshfree program uses several subroutines as illustrated in Figure 1.

In the case of a deterministic analysis, the stress will be directly used in the degradation model. Degradation model parameters (i.e. a_f and b_f) are calculated using the correction factors, S_u. Once the life of the component is calculated by the degradation model, the RUL after n_c cycles will be calculated. The framework continues this process k number of time steps until RUL ≤ 0 updating model parameters a_f and b_f with each time step, k. In the case of single amplitude loading, σ_a will be constant, whereas in the case of multiple amplitude loading, different σ_a values are passed from the meshfree model in every k. After the end of life, the framework provides a plot of RUL versus n_c.

In the case of probabilistic analysis, the framework uses σ_a from the meshfree model as a mean value and adds a customizable standard deviation to provide a PDF of stress values, which is used in the degradation model. The degradation model provides a PDF of the fatigue life and, hence, a PDF of the RUL can be obtained. Similar to the deterministic analysis, the parameters a_f and b_f are updated with every time step, k. Besides the PDF of σ_a is updated by using meshfree model in the case of multiple amplitude stress analysis. End of life criterion for the probabilistic prognostics is min(RUL) ≤ 0. The framework generates plots of PDF and CDF of RUL at every k and a plot of RUL versus n_c, depicting bounds of possible RUL with a customizable confidence interval.

Case Study – Fatigue Life of a Cantilever Beam

Meshfree Modeling

The model was initially constructed using 11×5 uniformly distributed nodes in the domain and along the boundaries to represent the 2D cantilever beam. However, to enhance model accuracy, 189 (21×9) nodes were used. Comparison with exact solution indicates that increased number of nodes improved the accuracy of results (i.e. y-displacement, normal and shear stresses). Increasing number of nodes to 189, however, increased the computational time of a 2.13 GHz processor to 7 minutes, which is a 400% increase. The greatest amount of computational time was consumed by the evaluation of the shape function, which was called by the main program and other subroutines 24,575 times and consumed 91% of the computational time. Therefore, efficient programming of the shape function subroutine plays a significant role in reducing computational time. Efficient shape function programming is especially useful for more complex shape functions such as those constructed using Moving Least Squares (MLS) method.

Results of the LRPIM were found to be highly sensitive to some of the model parameters such as factors that control the size of support domain, α_s, and that of the quadrature domain, α_q. Values of α_q were tested between recommended interval of 1.5 – 2.5 [29]. Best results were obtained at $\alpha_{qx} = \alpha_{qy} = \alpha_q = 1.7$. Optimum values of quadrature domains are essential to obtain accurate results. This is because $\alpha_q \leq 1$ makes the problem to behave like a strong form formulation, which has more errors. Too large α_q, on the other hand, yields erroneous solutions because of inaccurate integration caused by insufficient Gauss quadrature points. Nevertheless, using more Gauss quadrature points makes the program computationally expensive [29].

A rectangular support domain with $\alpha_s = 3$ was constructed around each node point for interpolation. With $\alpha_s = 3$, i.e. the size of the support domain three times that of the x and y nodal distances, the support domain encompassed sufficient field variables for interpolation. Because of its good capability of matrix operations, MATLAB was found to be helpful in

constructing an efficient program. Since the MATLAB program contains much less number of iteration loops and handles matrix math more effectively, it is computationally more efficient than the Fortran code by Liu and Gu [29]. The program was written as a function file so that it can easily be interfaced with the program for the degradation model. When called, the LRPIM program automatically transfers nodal displacements to the degradation model.

The stresses and deflections of the beam were verified using exact solutions. Figure 4 shows the *y*-deflection of the beam due to a parabolic traction with a pick value of 10 kN. As shown in the figure, the LRPIM solution shows good agreement with the exact solution. Bending stresses along the length of the beam are shown in Figure 5 depicting a good agreement with the exact solution. Shear stresses along the width of the beam are also compared with exact solution as shown in Figure 6.

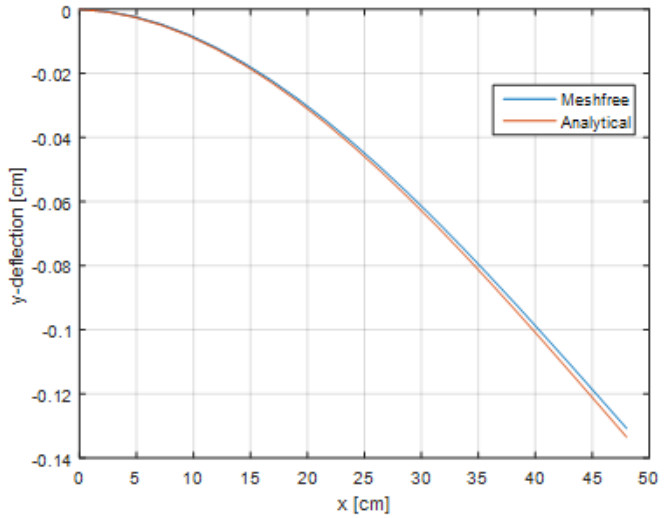

Figure 4. Vertical deflection of the beam at the central axis.

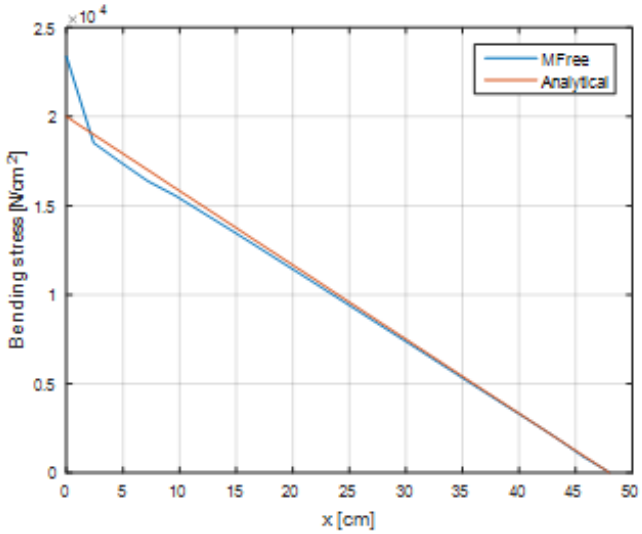

Figure 5. Bending stress along the length, *L*, of the beam.

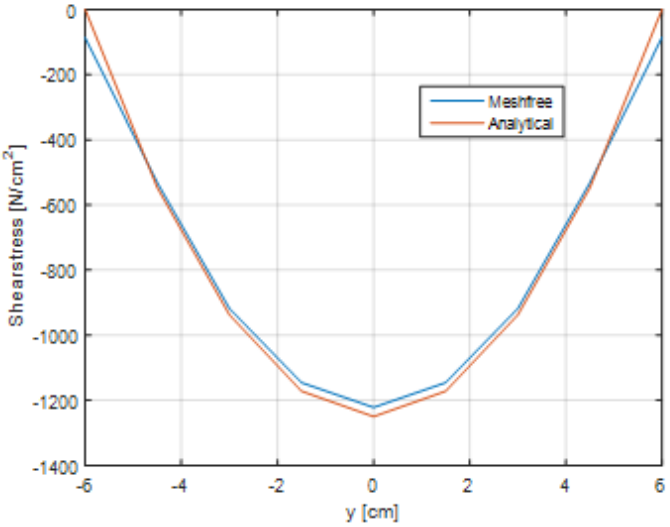

Figure 6. Variation of shear stress along the width of the beam.

LRPIM provides efficient way of modeling a physical problem that could easily be integrated with a degradation model in prognostics. The program for meshfree modeling was efficient and convenient as it is easy to alter values of parameters for model performance and accuracy. Verification with LRPIM solutions exhibits good agreement with those of exact solutions.

RUL Prediction

Deterministic RUL Prediction

Single amplitude loading and multiple amplitude loading cases were analyzed in the case of deterministic RUL prediction.

Single Amplitude Loadings

Considering an alternating stress, σ_a, of 200 MPa applied for 2×10^4 cycles, the life of the component was determined from *S-N* relationship. The correction factors, that are needed in Eq. (10c), were $C_L = 1$, $C_G = 0.7466$, $C_S = 0.5841$, $C_T = 0.71$and $C_R = 0.753$ [48][40]. This cyclic loading was applied consecutively for nine intervals. Because of a decrease in the endurance limit of the material due to CFD, the RUL decreases. Figure 7 shows the RUL of the beam until failure. The dotted black lines represent the original RUL plots for each cycle time whereas the blue bold zigzag line shows the actual trajectory of the RUL. It can be seen that initially the specimen was predicted to have a life of about 2.6×10^5 life cycles. It steps down to almost 2.4×10^5 after the first load application. Because of the change in the trajectory after each load application, however, it finally fails after only about 1.4×10^5 cycles. This value is 46% less than the total life originally estimated, i.e. 2.6×10^5 cycles. Although the stress level is the same, the CFD has caused the RUL to decrease. Note that without consideration of CFD, the RUL trajectory would follow the top dotted line in Figure 7. It is therefore, strongly recommended to consider CFD while calculating RUL.

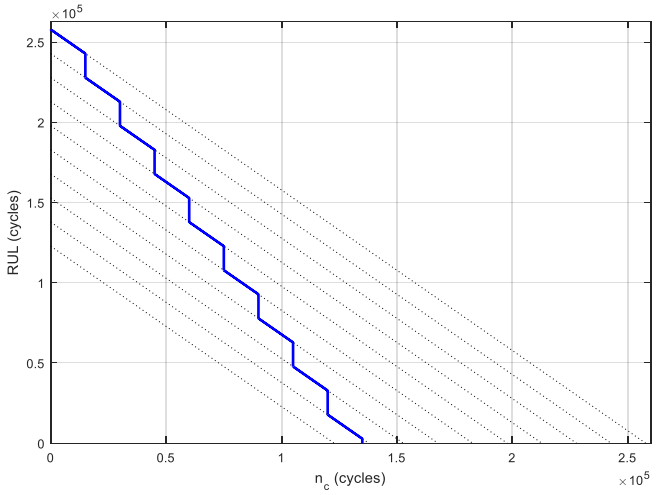

Figure 7. Nine consecutive constant stress of 200 MPa applied each for n_c = 1.5 x 10^4 cycles.

In this case, completely reversed stresses of ten different amplitudes, each applied for a total of $n_c = 1.5 \times 10^4$ cycles, were considered [40]. Figure 8 illustrates the true trajectory of the RUL when the beam is subjected to variable loading as depicted in the figure. Depending on the stress level, the lifecycle of the beam could increase or decrease. It could be observed that despite a decrease in the endurance limit, a decrease in the stress causes a relative increase of the RUL. Change in the stress amplitude alters the RUL trajectory as shown in Figure 8. Each segment of the RUL corresponds to each loading cycle of the component. The initial life of the beam was estimated from the *S-N* relationship to be about 2.6×10^5 cycles. Due to a 200 MPa load application for 1.5×10^4 cycles, the RUL shows a decrease as depicted in the first segment of the zigzag line. After the beam was subjected to the initial loading of 200 MPa, the load was increased to 250 MPa. The increased loading as well as the CFD cause the RUL to drop to 1.5×10^5cycles. The RUL follows this trajectory for the next 1.5×10^4 cycles until it increases to about 2.7×10^4 cycles due to a decrease of stress to 150 MPa. The last stress was applied for 9×10^4 cycles until the beam fails after a total of 2.2×10^5 cycles.

Multiple Amplitude Loadings

Deterministic analyses using the framework under single mean and multiple mean loadings depict that CFD plays a significant role in RUL predictions of a system undergoing cyclic loadings. It was also shown that the amplitude of the stress can change the trajectory of the RUL and the system may fail in less number of cycles than what was predicted during initial loading. Therefore, it is crucial to continuously estimate the magnitude of future loading and to quantify its uncertainty to accurately predict RUL.

Probabilistic RUL Prediction

As in the case of deterministic RUL prediction, multiple applications of cyclic loads were employed until failure. However, in the case of a probabilistic RUL prediction, the loads considered at each level are probabilistic, represented by a PDF. In other words, samples of stresses for each level of load application were generated using a Gaussian (normal) PDF with the deterministically evaluated stresses from meshfree model as mean values and a standard deviation of 10% of the mean value. Results of consecutive load applications of single mean value and multiple mean values are presented.

Loadings of Single Mean Value

A single mean value was used to generate six stress PDFs to study the effect of CFD due to consecutive loading conditions. Application of the first stress PDF (Figure 9) to the framework provides a PDF of the RUL. Application of the second stress PDF will cause the mean of the PDF of the RUL to decrease. Similarly, further applications of the stress PDFs will cause the mean of the RUL to gradually decrease to zero.

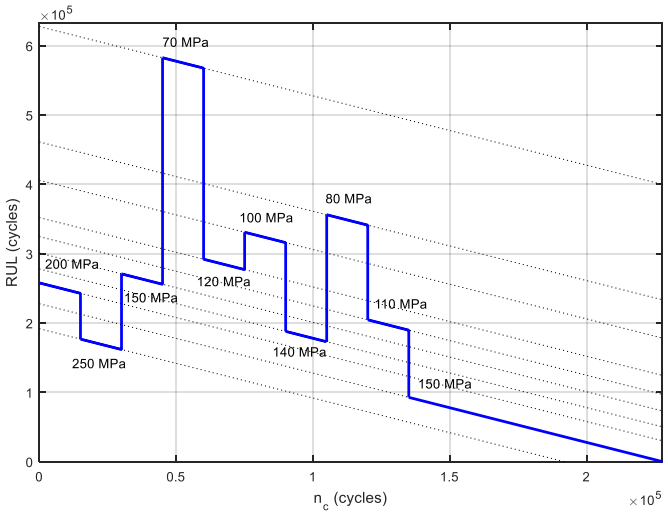

Figure 8. Consecutive variable stress application each for n_c = 1.5 x 10^4 cycles.

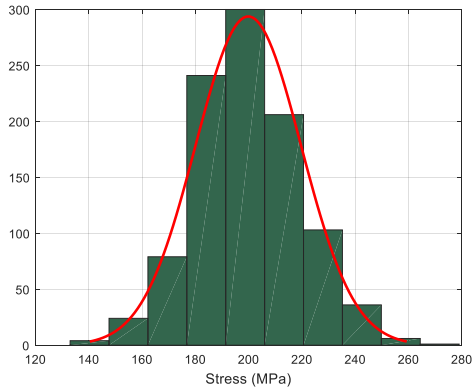

Figure 9. Stress distribution with a mean of 200 MPa and a 10% standard deviation.

Figure 10 shows the PDF and CDF of the initial predicted life of the beam. Similarly, PDFs and CDFs of RUL at each level

of load application until failure can be obtained. These levels of load applications are discussion hereunder. Figure 10 shows the PDF and CDF of the initial fatigue life of the beam depicting a range of RUL values. The CDF shows the probability of occurrence of a particular RUL value or less. For instance, it can be observed from the CDF in Figure 10 (a) that initially there is a 70% probability that the RUL of the beam would be about 2.5×10^5 cycles or less.

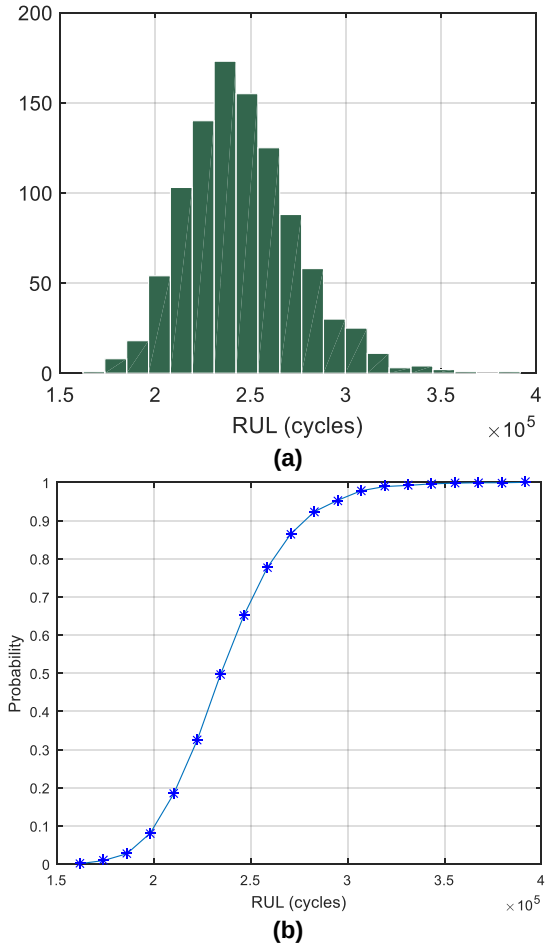

Figure 10. (a) CDF of initial life, (b) PDF of initial life.

RUL values of the median and 98% bounds of confidence level were plotted in Figure 11. The size of the bounds implies that the level of uncertainty of RUL prediction is high at the beginning and decreases towards the end of life. Probabilistic prognostics accounts for uncertainty, and hence, encompasses a range of possible RUL values that enable the engineer to predict the status of a component more confidently.

Loadings of Multiple Mean Values

Stress values from variable loading cases of deterministic analyses were used as mean values to generate seven normal distributions with different mean values and coefficient of variation of 0.1. Each case of variable cyclic loading was applied for 1.5×10^4 cycles. The magnitude of the stress is inversely related to the RUL. Therefore, RUL could generally increase or decrease from its previous estimated value depending on the magnitude of the stress. PDFs of stresses were used consecutively to generate RUL values after each case of cyclic load application. Figure 12 shows the median RUL and its 98% bounds of confidence level. It can be seen from the figure that, the RUL changes inversely with the mean amplitude of the stresses. The RUL provides a better RUL estimation showing a range of possible outcomes under six discrete mean values of variable cyclic loading cases each applied for 1.5×10^4 cycles.

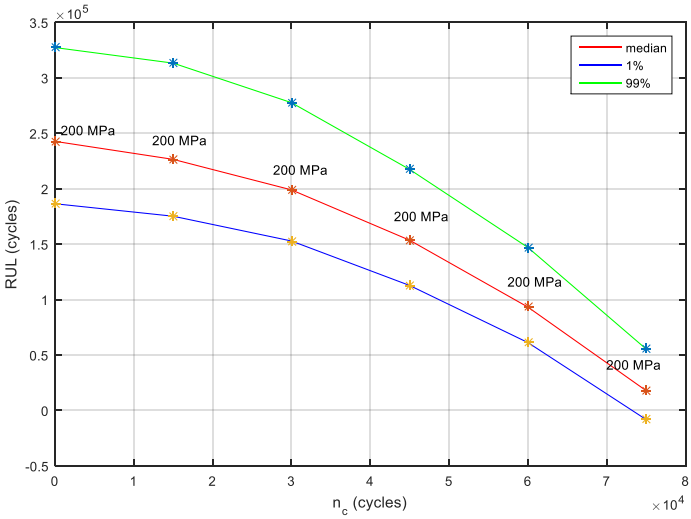

Figure 11. RUL values showing the median and 98% bounds of confidence level.

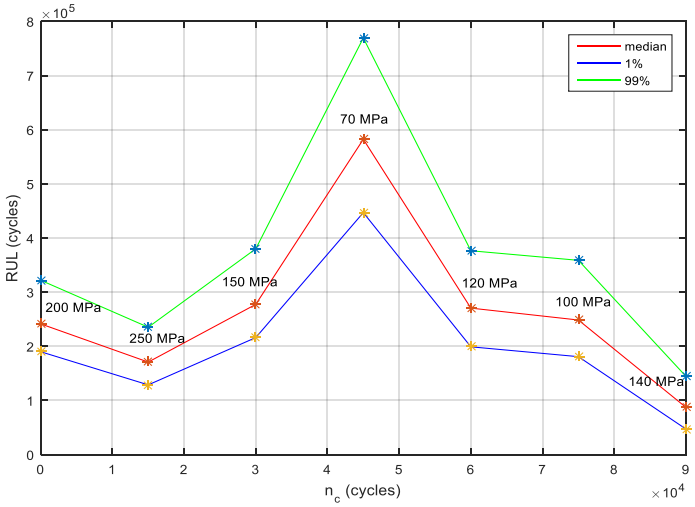

Figure 12. Trajectory of RUL lines showing 98% confidence interval.

Probabilistic analyses of single and multiple mean amplitude values provided better RUL predictions by

considering the loading uncertainty. The probabilistic analysis not only provides a range of possible RUL values but it also provides the probability of obtaining a specific RUL value at each level in the life of a component. However, probabilistic analysis requires PDF values of random variables, which can increase the computation time. Therefore, it is important to investigate computationally efficient methods for probabilistic analysis. To this end, probabilistic analysis using FORM and MC method are compared hereunder.

Efficient Probabilistic Analysis

In order to implement a computationally efficient probabilistic analysis into the prognostics framework, the FORM was investigated to compute the initial life of the beam. Considering two random variables (i.e. σ_a and S_u), the results of the FORM were compared with that of MC method of 10,000 samples. Comparison of the CDFs shown in Figure 13 depicts that results of the FORM are in good agreement with that of MC method. However, the accuracy of MC method relies on a large sample size, which makes the analysis computationally expensive especially for complex problems. It was observed that MC sampling using 10,000 samples requires 250% increase in computational time than that of FORM. It is, thus, more efficient to employ FORM to perform a probabilistic analysis for such applications.

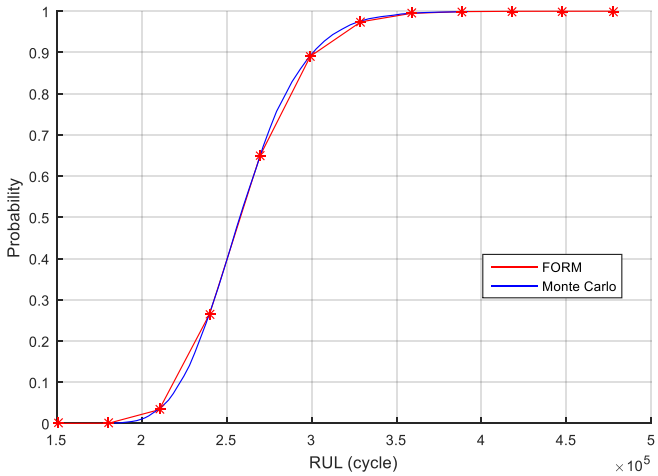

Figure 13. CDF of RUL using FORM and MC methods.

The sensitivity of the RUL to each random variable is shown in Figure 14. The red bars represent sensitivities of the RUL with respect to the mean values of the random variables, whereas the blue ones represent sensitivities with that of the standard deviations. The mean sensitivity values depict that the stress (σ_a) has a positive sensitivity implying that the probability of failure increases (i.e. reliability decreases) with increasing stress. On the other hand, the ultimate strength (S_u) has a negative relationship since the probability of failure decreases with increasing S_u. Besides, from the height of the sensitivity levels it can be deduced that the RUL is more sensitive to the stress than the ultimate strength. Thus, for a longer RUL, a reduction of stress amplitude will be more effective.

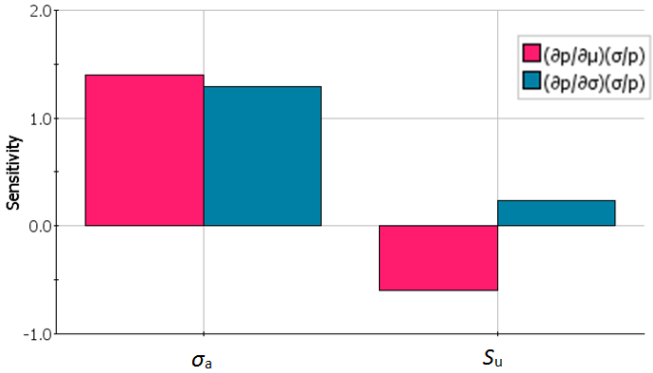

Figure 14. Sensitivity levels of stress (σ_a) and ultimate strength (S_u) using FORM.

CONCLUSIONS

In this paper, meshfree modeling was implemented in model-based probabilistic prognostics to efficiently predict RUL. A computational framework for predicting the RUL of a component under fatigue loading was developed. The framework is capable of predicting RUL both deterministically and probabilistically. Besides, the framework consists of meshfree modeling algorithm that is efficient with customizable parameters that enhance model performance and accuracy. Verification with LRPIM solutions exhibits good agreement with those of exact solutions. The meshfree program could be replaced by other meshfree methods that are based on local weak-forms, such as MLPG method, by replacing the LRPIM shape function with MLS shape function. The computational framework aids in decision making and fault mitigation. As a case study, the framework was implemented to investigate the RUL of a cantilever beam under fatigue loading.

Deterministic analyses of the case study model under constant and variable loadings depict that CFD plays a significant role in RUL predictions of a system undergoing cyclic loadings. Probabilistic RUL analyses generated a probability of getting a certain RUL value at any instant during the lifetime of the cantilever beam. It was also shown that the amplitude of the stress can change the trajectory of the RUL and the system may fail in less number of cycles than what was predicted during initial loading. Therefore, it is crucial to continuously estimate the magnitude of future loading and to quantify its uncertainty to accurately determine the path of the RUL lines. Probabilistic prognostics results show a range of possible RUL values so that a decision will be made to deter failure and avoid downtime. Comparison of the MC method and FORM for probabilistic analysis shows that FORM is significantly computationally efficient and provides results which are in good agreement with those of MC method. Two random variable probabilistic analyses showed that RUL is more sensitive to the stress level than the ultimate strength of the material.

NOMENCLATURE

b	External force vector
$\boldsymbol{B}$	Strain matrix
B	Width of cantilever
C_G	Size factor
C_L	Loading factor
C_R	Reliability factor
C_S	Surface factor
C_T	Temperature factor
CDF	Cumulative Distribution Function
CFD	Cumulative Fatigue Damage
D	Matrix of elastic constants
d_{cl}	Distance between nodes
E	Young's modulus
$\boldsymbol{f}$	Nodal force vector
FEM	Finite Element Method
H	Height of cantilever
k	Time step
$\boldsymbol{K}$	Nodal stiffness matrix
L	Length of cantilever
LRPIM	Local Radial Point Interpolation Method
MLPG	Meshless Local Petrov-Galerkin
MLS	Moving Least Squares
N	Number of life cycles available
n	Number of nodes
$\boldsymbol{n}$	Unit normal vector
n_c	Number of cycles of loading
p	A vector of basis functions
PDF	Probability Density Function
r	Number of applied loads
RUL	Remaining Useful Life
r_q	Size of local quadrature domain
r_s	Size of support domain
r_w	Size of weight domain
S_e	Endurance limit
S_m	Mean stress
S_u	Ultimate stress
t	Traction on boundary
u	Field variable
V	Matrix of weight derivatives
v	Nodal displacement in y-direction
$\widehat{\boldsymbol{W}}$	Weight function
X-FEM	eXtended Finite Element Method
x_Q	Gauss quadrature point
α_q	Non dimensional parameter that controls size of quadrature domain
α_s	Non dimensional parameter that controls size of support domain
$\boldsymbol{\varepsilon}$	Strain
Γ	Global boundary
Γ_{qi}	Boundary that does not intersect with the global boundary
Γ_{qt}	Boundary that intersects with the natural boundary
Γ_{qu}	Boundary that interests with the essential boundary
υ	Poisson's ratio
$\boldsymbol{\sigma}$	Stress tensor
σ_a	Alternating stress
φ	Shape function
Ω	Global domain
Ω_q	Local quadrature domain

REFERENCES

[1] Garga, A. K., McClintic, K. T., Campbell, R. L., Yang, C.-C., Lebold, M. S., Hay, T. a., and Byington, C. S., 2001, "Hybrid reasoning for prognostic learning in CBM systems," 2001 IEEE Aerosp. Conf. Proc. (Cat. No.01TH8542), **6**, pp. 2957–2969.

[2] Bartram, G. W., 2013, "System Health Diagnosis and Prognosis Using Dynamic Bayesian Networks."

[3] Sankararaman, S., 2015, "Significance, interpretation, and quantification of uncertainty in prognostics and remaining useful life prediction," Mech. Syst. Signal Process., **52-53**, pp. 228–247.

[4] Pecht, M. G., 2013, "Solid State Lighting Reliability: Components to Systems," W.D. van Driel, and X.J. Fan, eds., Springer New York, New York, NY, pp. 373–393.

[5] Sankararaman, S., and Goebel, K., 2014, "An Uncertainty Quantification Framework for Prognostics and Condition-Based Monitoring," 16th AIAA Non-Deterministic Approaches Conf., pp. 1–9.

[6] Bartram, G., and Mahadevan, S., 2015, "Probabilistic Prognosis with Dynamic Bayesian Networks," Int. J. Progn. Heal. Manag., pp. 1–23.

[7] An, D., Choi, J. H., and Kim, N. H., 2013, "Prognostics 101: A tutorial for particle filter-based prognostics algorithm using Matlab," Reliab. Eng. Syst. Saf., **115**, pp. 161–169.

[8] Liu, J., Saxena, A., Goebel, K., Saha, B., and Wang, W., 2010, "An Adaptive Recurrent Neural Network for Remaining Useful Life Prediction of Lithium-ion Batteries," pp. 0–9.

[9] Saha, B., Goebel, K., and Christophersen, J., 2009, "Comparison of prognostic algorithms for estimating remaining useful life of batteries," Trans. Inst. Meas. Control, **31**(3-4), pp. 293–308.

[10] Si, X. S., Wang, W., Hu, C. H., and Zhou, D. H., 2011, "Remaining useful life estimation - A review on the statistical data driven approaches," Eur. J. Oper. Res., **213**(1), pp. 1–14.

[11] Heng, A., Zhang, S., Tan, A. C. C., and Mathew, J., 2009, "Rotating machinery prognostics: State of the art, challenges and opportunities," Mech. Syst. Signal Process., **23**(3), pp. 724–739.

[12] An, D., Kim, N. H., and Choi, J. H., 2015, "Statistical aspects in neural network for the purpose of prognostics," J. Mech. Sci. Technol., **29**(4), pp. 1369–1375.

[13] An, D., Kim, N. H., and Choi, J. H., 2015, "Practical options for selecting data-driven or physics-based prognostics algorithms with reviews," Reliab. Eng. Syst. Saf., **133**, pp. 223–236.

[14] Tian, Z., Jin, T., Wu, B., and Ding, F., 2011, "Condition based maintenance optimization for wind power generation systems under continuous monitoring," Renew. Energy, **36**(5), pp. 1502–1509.

[15] Sikorska, J. Z., Hodkiewicz, M., and Ma, L., 2011, "Prognostic modelling options for remaining useful life estimation by industry," Mech. Syst. Signal Process., **25**, pp. 1803–1836.

[16] Saxena, A., Celaya, J., Saha, B., Saha, S., and Goebel, K., 2010, "Evaluating prognostics performance for algorithms incorporating uncertainty estimates," IEEE Aerosp. Conf. Proc.

[17] Saxena, A., Celaya, J. R., Saha, B., Saha, S., and Goebel, K., 2009, "On Applying the Prognostic Performance Metrics," Proc. Annu. Conf. Progn. Heal. Manag. Soc., pp. 1–16.

[18] Saxena, A., Celaya, J., Saha, B., Saha, S., and Goebel, K., 2010, "Metrics for Offline Evaluation of Prognostic Performance," Int. J. Progn. Heal. Manag., (1), pp. 1–20.

[19] Zhao, F., Tian, Z., and Zeng, Y., 2013, "A stochastic collocation approach for efficient integrated gear health prognosis," Mech. Syst. Signal Process., pp. 1–16.

[20] Daigle, M., Saxena, A., and Goebel, K., 2012, "An efficient deterministic approach to model-based prediction uncertainty estimation," Annu. Conf. Progn. …, pp. 1–10.

[21] Zhao, F., Tian, Z., and Zeng, Y., 2013, "Uncertainty Quantification in Gear Remaining Useful Life Prediction Through an Integrated Prognostics Method," IEEE Trans. Reliab., **62**(1), pp. 146–159.

[22] Sankararaman, S., and Goebel, K., 2013, "Why is the Remaining Useful Life Prediction Uncertain ?," Annu. Conf. Progn. Heal. Manag. Soc. 2013, pp. 1–13.

[23] Sankararaman, S., Daigle, M. J., and Goebel, K., 2014, "Uncertainty Quantification in Remaining Useful Life Prediction Using First-Order Reliability Methods," IEEE Trans. Reliab., **63**(2), pp. 1–17.

[24] Chaari, F., Fakhfakh, T., and Haddar, M., 2009, "Analytical modelling of spur gear tooth crack and influence on gearmesh stiffness," Eur. J. Mech. A/Solids, **28**(3), pp. 461–468.

[25] Rao, B. N., and Rahman, S., 2000, "An efficient meshless method for fracture analysis of cracks," Comput. Mech., **26**(4), pp. 398–408.

[26] Liu, F., and Borja, R. I., 2008, "A contact algorithm for frictional crack propagation with the extended finite element method," Int. J. Numer. Methods Eng., **76**, pp. 1489–1512.

[27] Nguyen, V. P., Rabczuk, T., Bordas, S., and Duflot, M., 2008, "Meshless methods: A review and computer implementation aspects," Math. Comput. Simul., **79**(3), pp. 763–813.

[28] Chaari, F., Fakhfakh, T., and Haddar, M., 2009, "Analytical modelling of spur gear tooth crack and influence on gearmesh stiffness," Eur. J. Mech. A/Solids, **28**(3), pp. 461 – 468.

[29] Liu, G. R., and Gu, Y. T., 2005, An introduction to meshfree methods and their programming, Springer, Dordrecht, The Netherlands.

[30] Bordas, S., Nguyen, P. V., Dunant, C., Nguyen-dang, H., and Guidoum, A., 2006, "An extended finite element library," Int. J. Numer. Meth. Engng., **41**(0), pp. 1–33.

[31] Liu, G. R., 2010, Meshfree methods: moving beyond the finite element method, CRC Press, Boca Raton.

[32] Belytschko, T., Gu, L., and Lu, Y. Y., 1999, "Fracture and crack growth by element free Galerkin methods," Model. Simul. Mater. Sci. Eng., **2**(3A), pp. 519–534.

[33] Atluri, S. N., and Zhu, T., 1998, "A new Meshless Local Petrov-Galerkin (MLPG) approach in computational mechanics," Comput. Mech., **22**(2), pp. 117–127.

[34] Lee, S. J., Zi, G., Mun, S., Kong, J. S., and Choi, J. H., 2015, "Probabilistic prognosis of fatigue crack growth

for asphalt concretes," Eng. Fract. Mech., **141**, pp. 212–229.

[35] Zio, E., and Peloni, G., 2011, "Particle filtering prognostic estimation of the remaining useful life of nonlinear components," Reliab. Eng. Syst. Saf., **96**(3), pp. 403–409.

[36] An, D., Choi, J.-H., and Kim, N. H., 2012, "Identification of correlated damage parameters under noise and bias using Bayesian inference," Struct. Heal. Monit., **11**(3), pp. 293–303.

[37] Dong, L., Haynes, R., and Atluri, S. N., 2015, "On improving the celebrated Paris' power law for fatigue, by using moving least squares," Comput. Mater. Contin., **45**(1), pp. 1–15.

[38] Cox, B. N., Gao, H., Gross, D., and Rittel, D., 2005, "Modern topics and challenges in dynamic fracture," J. Mech. Phys. Solids, **53**(3), pp. 565–596.

[39] Daigle, M., Kulkarni, C. S., and Gorospe, G., 2014, "Application of model-based prognostics to a pneumatic valves testbed," IEEE Aerosp. Conf. Proc., (Dv).

[40] Ekwaro-Osire, S., Endeshaw, H. B., Pham, D. H., and Alemayehu, F. M., 2015, "Uncertainty in remaining useful life prediction," 23rd ABCM International Congress of Mechanical Engineering, Rio de Janeiro.

[41] Haldar, A., and Mahadevan, S., 2000, Probability, Reliability and Statistical Methods in Engineering Design, John Wiley & Sons, Inc.

[42] Alemayehu, F. M., and Ekwaro-Osire, S., 2011, "Probabilistic Multibody Modeling of Gearboxes for wind turbines," Proceedings of the ASME IMECE2011, Denver, Colorado.

[43] Alemayehu, F. M., and Ekwaro-Osire, S., 2012, "Uncertainty Considerations in the Dynamic Loading and Failure of Gear Pairs," J. Mech. Des., (Under Review).

[44] Alemayehu, F., and Ekwaro-Osire, S., 2014, "Loading and Design Parameter Uncertainty in the Dynamics and Performance of High-Speed-Parallel-Helical Stage of a Wind Turbine Gearbox," J. Mech. Des., **136**(9), pp. 1–13.

[45] Alemayehu, F. M., and Ekwaro-Osire, S., 2015, "Probabilistic Performance of Helical Compound Planetary System in Wind Turbine," J. Comput. Nonlinear Dyn., **10**(4), p. 041003.

[46] Li, C. J., and Lee, H., 2005, "Gear fatigue crack prognosis using embedded model, gear dynamic model and fracture mechanics," Mech. Syst. Signal Process., **19**(4), pp. 836–846.

[47] Tian, Z., 2009, "An artificial neural network method for remaining useful life prediction of equipment subject to condition monitoring," J. Intell. Manuf., **23**(2), pp. 227–237.

[48] Juvinall, R., and Marshek, K. ., 2000, Fundamentals of Machine Components Design, New York.

[49] Budynas, R., and Nisbett, K., 2014, Mechanical Engineering Design, Mc-Graw Hill.